Review of Recent Trends in Design of Traction Inverters for Electric Vehicle Applications

Chandra Sekhar Goli[1], Somasundaram Essakiappan[2], Prasanth Sahu[3], Madhav Manjrekar[1,2] Nakul Shah[3]
[1]Department of Electrical and Computer Engineering, University of North Carolina at Charlotte, USA
[2] Energy Production and Infrastructure Center, University of North Carolina at Charlotte, USA
[3]QM Power Inc, Charlotte, USA

***Abstract*- A surge in usage of electric vehicles in transportation sector over the past decade is overwhelming. Recent trends in the design of traction inverters employed in commercially available electric vehicle (EV) traction applications have been reviewed in this paper. A trend in design matrices namely Volumetric Power Density (VPD) in kW/L and Gravimetric Power Density (GPD) in kW/kg of different traction inverters have been presented. A standard topology of the traction inverter and control methodology employed in EV applications have been reviewed. The selection of the components to meet the targets of design matrices set by the United States, Department of Energy (DoE) has been discussed. Thus, the paper provides a useful reference for original equipment manufacturers.**

Keywords-traction inverter, electric vehicle, transportation

I. INTRODUCTION

The current state of the art of traction motors has been reviewed in this section. A handout [1] from the U.S. Department of Energy (DoE) has listed key targets for traction motor and Power Electronics Inverter Module (PIM) of the electric drive system for the years 2020 and 2025 are shown in TABLE.1 and TABLE 2.

TABLE 1: DOE TARGETS FOR TRACTION MOTOR AND PIM [1]

DoE Targets	Cost ($/kW)		Power Density (kW/L)	
	2020	2025	2020	2025
Traction Motor	4.7	3.3	5.7	50
PIM	3.3	2.70	13.4	100

DoE targets for key electrical and thermal specifications have been listed in TABLE 2.1 and TABLE 2.2.

TABLE.2.1: DOE TARGETS FOR KEY ELECTRIC SPECIFICATIONS [1]

Peak Power (kW)	200
Continuous Power (kW)	110
Battery Operating Voltage (V_{dc})	850-1100
Voltage Rating (V)	1200
Maximum Device Current (A)	200
Maximum Current (A)	800
Switching Frequency (kHz)	30-50
Maximum Efficiency	>98
Power Factor	>0.6

TABLE 3: SPECIFICATIONS OF COMMERCIALLY AVAILABLE TRACTION INVERTERS [2-14]

	EV Type	Motor Type	Power (kW or kVA)	DC Link Voltage (V)	VPD (kW/L)	GPD (kW/kg or kVA/kg**)	Device	Cooling Methodology
Jaguar I-Pace 2019 [2]	BEV	PMSynRM	300* kW	500	32.68	36.45	Si IGBT	Water-Glycol
Nissan Leaf 2019 [2]	BEV	PMSynRM	140* kW	450	4.21*	12.55	Si IGBT	Water-Glycol
Tesla M3 2018 [2]	BEV	PMSynRM IM	344* kW	430	27.4*	71.51**	SiC MOSFET	Water-Glycol
Chevy Bolt 2017 [3]	BEV	PMSynRM	153 kVA	350	19.61*	15.93*	Si IGBT	Water-Glycol
Toyota Prius 2016 [4]	PHEV	PMSynRM	162.2* kW	600	11.5	16.7	Si IGBT	-
Audi e-Tron 2016 [2]	PHEV	IM, IM	75* kW	600	9.375	7.5	Si IGBT	Double Sided WEG
BMW i3 2016 [4]	BEV	PMSynRM	125	355	9.375	14.1	Si IGBT	-
Chevy Volt 2016 [5]	PHEV	PMSynRM	180*	360	17.3*	21.7**	Si IGBT	Double Sided WEG
Cadillac CT6 2016 [6]	PHEV	IPMSM	215*	360	23*	16.5**	Si IGBT	Double Sided WEG
Tesla S 2015 [6]	BEV	-	320* kW	430	47-50*	52-55*	Si IGBT	-
Honda Accord 2014 [4]	HEV	IPMSM	-	700	-	-	Si IGBT	-
Chevy Spark 2014 [3]	BEV	PMSM	140 kVA	350	10.68*	10.29**	Si IGBT	-
Toyota Camry 2013 [4]	HEV	PMSynRM	-	650	11.5	12.7	Si IGBT	WEG
Nissan Leaf 2012 [6]	BEV	PMSynRM	80 kW	375	7.1	4.94	-	-
Sonata HSG 2012 [4]	HEV	PMSM	23 kW	270	7.3	6.9	Si IGBT	Ethylene Glycol
Toyota Prius 2010 [7]	HEV	IPMSM	-	650	5.9	6.9	Si IGBT	Water-Glycol
Lexus 2008 [7]	HEV	IPMSM	-	650	10.6	7.7	Si IGBT	Double Sided W-G
Toyota Camry 2007 [4]	HEV	IPMSM	70 kW(peak)	650	11.7	9.3	Si IGBT	Water-Glycol
Honda Accord 2006 []	HEV	PMSM	12 kW	-	2.4	2.9	Si IGBT	Air cooled Heat Sink
Toyota Prius 2004 [7]	HEV	IPMSM	50 kW	500	3.8	4.5	Si IGBT	Water-Glycol

-unknown, *estimated, IM: Induction Motor, PMSynRM: Permanent Magnet Assisted Synchronous Reluctance Machine, IPMSM: Internal Permanent Magnet Machine, W-G: Water-Glycol, WEG: Water-Ethylene-Glycol

This project was supported by U.S. Department of Energy award DE-EE0008871.

978-0-7381-4237- 1/21/$31.00 ©2021 IEEE

TABLE.2.2: DOE TARGETS FOR KEY THERMAL SPECIFICATIONS [1]

Maximum Junction Temperature (°C)	250
Ambient Operating Temperature (°C)	-40 to +125
Storage Temperature (°C)	-40 to +125
Maximum Cooling System Flow Rate (lpm)	10
Maximum Coolant Inlet Temperature (°C)	85
Maximum Inlet Pressure (Psi)	25
Maximum Inlet Pressure Drop (Psi)	>98
Volume (liters)	2
Mass (kg)	4

This reference may provide an opportunity for the research community of Original Equipment Manufacturers (OEM) and academia to enhance the infrastructure of electric mobility. These targets have been set to envision an extended range in mileage of the electric vehicles by improving the performance of the various components involved in electric vehicle traction applications at the device level.

Several reviews of state of the art of traction inverter have highlighted the necessity of wide bandgap (WBG) devices to meet the higher switching frequency requirements have been focused on either all-electric or plug-in hybrid or hybrid vehicles [15][16]. Different topologies of traction inverters and power electronic components employed in battery-operated electric vehicles and hybrid electric vehicles at General Motors have been reviewed in numerous papers [17-19]. However, a trend in key design matrices of traction inverters hasn't been reviewed extensively in the existing literature. An extensive list of specifications of traction inverters employed in Battery

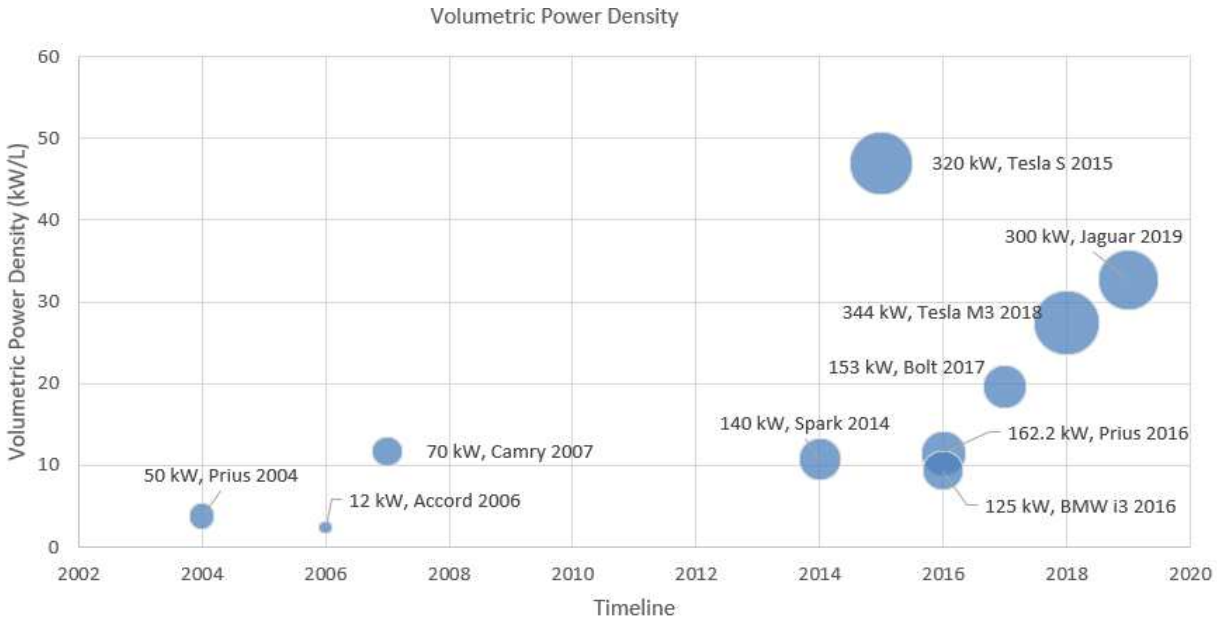

Figure.1. Trend in volumetric power density of commercially available traction inverters from the year 2004 to 2020 [2-14].

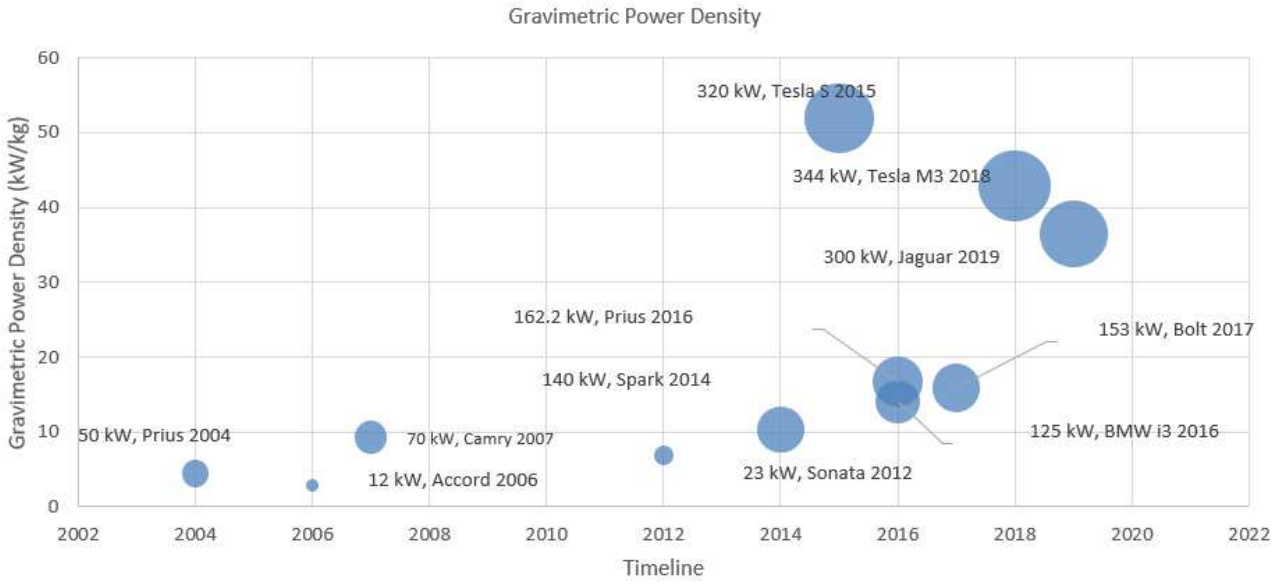

Figure.2. Trend in gravimetric power density of commercially available traction inverters from the year 2004 to 2020 [2-14].

Operated Electric Vehicles (BEV), Hybrid Electric Vehicles (HEV), Plugin Hybrid Electric Vehicles (PHEV), and Fuel Cell Electric Vehicles (FCEV) have been reviewed in this paper. Key specifications of electric vehicles listed in TABLE 3 have been profiled based on Volumetric Power Density (VPD) and Gravimetric Power Density (GPD) as shown in figure.1 and figure. 2. Area of the bubble in the plot is proportional to the power rating of the traction inverter. A power factor of 0.6 has been considered to estimate the kW rating of the traction inverter.

II. Topology and Control Methodology

The circuit topology of the traction inverter is decided based on the winding topology of the traction motor. Dual inverter topology would be preferred for open-ended winding with six terminals out [20]. Asymmetrical bridge inverter topology is used in the case of switched reluctance motors [21]. Classic three-phase traction inverter topology is suitable to drive AC traction motors. The three-phase inverter topology with a fewer number of switching devices is good to improve the VPD and GPD but a dual inverter topology with an optimized package would double the VPD and GPD [22]. The control methodology has been shown in Fig.3, has an outer speed loop, torque loop, and inner current loops. Maximum Torque Per Ampere (MTPA), and Field Weakening (FWA) control are the two proven methods to regulate the speeds below the rated speed and below the rated speed [23-25]. Static torque test or locked rotor test and back EMF test or open circuit tests are performed on traction motor to determine torque constant in N/m and speed constant V/rpm. The torque constant and speed constants are embedded into MPTA and FWA control algorithms.

The traction motors must have to be operated over a wide range of speeds in the constant power region. Thus, operating currents and voltages of traction motors would be at higher frequencies, demand higher switching frequency operation of

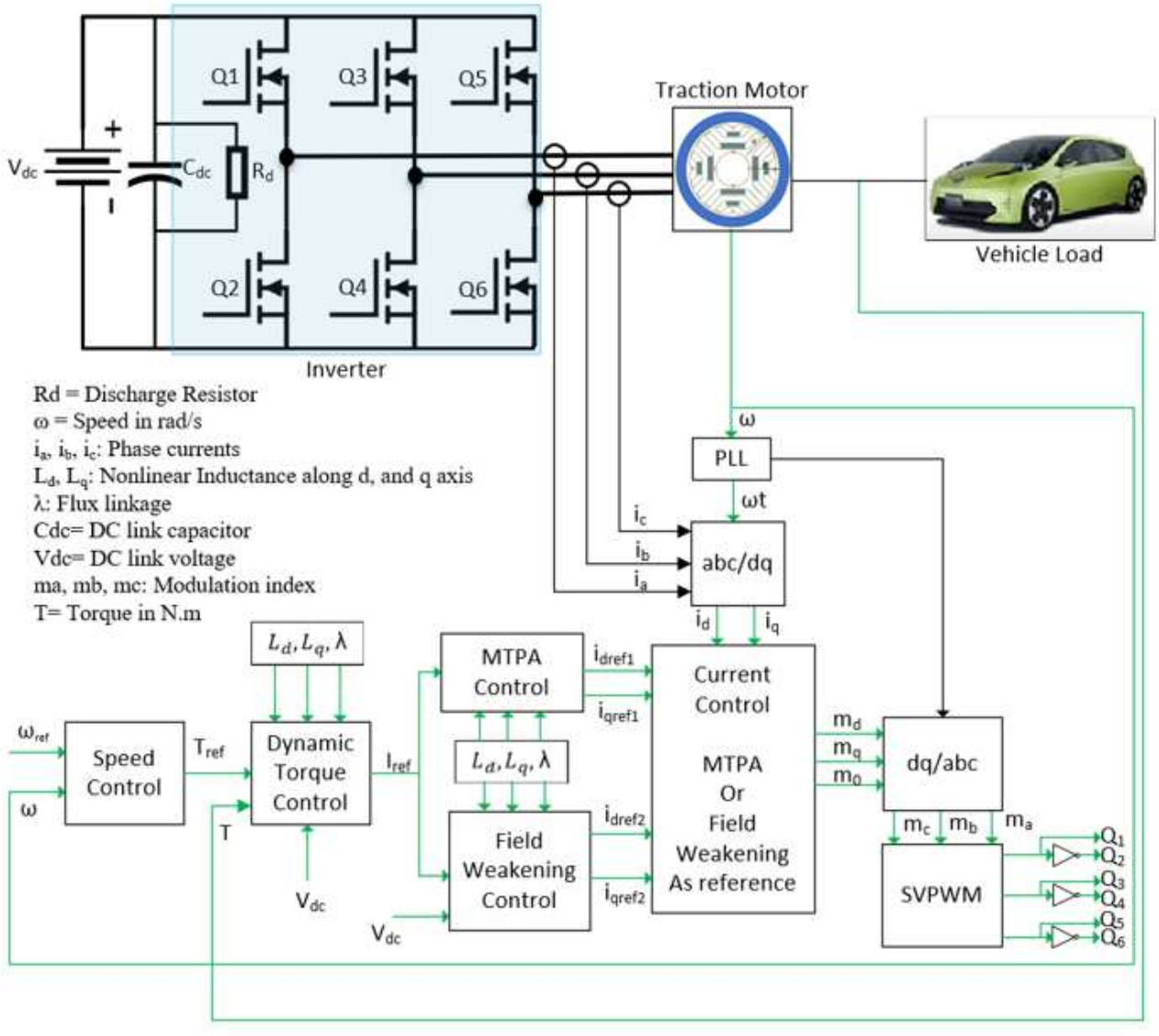

Figure.3. Simplified schematic of speed and torque control block diagram of traction inverter.

traction inverter. Sampling rates of the phase currents have to be set properly to operate the traction inverter in the stable mode for a wide range of speeds, and torques. The fundamental frequency of traction motor is higher than the conventional motor, would demand higher switching frequencies, and thus demand higher sampling rates of current and subsequent outer loops. The sampling rate criteria for the various control loops involved in the design of speed and torque control of the traction motor may have to comply with sampling frequencies defined in equations (1) to (5).

$$\text{Current loop sampling frequency}(f_i) = f_{sw} \quad (1)$$

$$\text{Speed loop sampling frequency}(f_n) = \frac{1}{5} \times f_{sw} \quad (2)$$

$$\text{Current loop cross over frequency}(f_{cri}) == \frac{1}{10} \times f_{sw} \quad (3)$$

$$\text{Speed loop cross over frequency}(f_{crn}) == \frac{1}{10} \times f_{cri} \quad (4)$$

$$\text{Torque loop cross over frequency}(f_{crn}) == \frac{1}{10} \times f_{cri} \quad (5)$$

MTPA and FWA controller generates a pair of d-axis and q-axis currents which have been fed to the inner current control loop. Inner current controller loops must be sampled at the switching frequency of the inverter. A flag has been set to choose the reference signals of currents either from the MTPA controller or FWA controller based on the speed and torque requirements. The inner current controller chooses the reference currents generated by the MTPA controller for below-rated speeds or else reference currents generated by the FWA controller will be fed to the inner current controller.

Characteristics of permanent magnet-based traction motor are defined by current and flux dependent instantaneous voltage equations (6) and (7). Voltage and current ratings of traction inverter are limited by either maximum ratings of motor or inverter whichever is lower as per boundary conditions defined by equations (8) and (9).

$$V_d = r_s I_d + L_d \frac{dI_d}{dt} - \omega_e L_q I_q \quad (6)$$

$$V_q = r_s I_q + L_q \frac{dI_q}{dt} - \omega_e (L_d I_d + \lambda_{pm}) \quad (7)$$

$$I_d{}^2 + I_q{}^2 \leq I_{peak}{}^2 \quad (8)$$

$$V_d{}^2 + V_q{}^2 \leq V_{peak}{}^2 \quad (9)$$

Boundary conditions of the traction motor drive system are influenced by cooling methodology. Liquid cooling of traction motor and inverter have been employed in electric vehicles to operate the motor-drive system at higher current densities to utilize the maximum torque range of the motor.

The MTPA control algorithm is implemented during the starting phase of the motor to meet high torque requirements. A transition from MTPA control to FWA control will happen as the speed increases beyond rated speed. However, the output power of the traction motor is limited by compromising torque at very high speeds during FWA control. The maximum torque per voltage (MTPV) control algorithm could enhance the output power at higher speeds without limiting the torque despite the increase in speed [27, 28]. Thus, optimal performance of traction drive system can be achieved by inclusion MTPV control algorithm in addition to MTPA and FWA control.

III. Selection of Components

A. Busbars

The power loop inductance of the traction inverter affects the switching frequency and thus the speed control as well. Loop inductance may cause a delay in turn on and turn off times of switching devices. A small delay in turn on or turn off switching times of MOSFET severely affects the operation of traction inverter at higher frequencies [29]. Laminated busbars of a thin layer of metals separated by insulating material would significantly reduce the loop inductance, enhances the stability of the controller, and improves the power density as well. The laminated busbars can be customized as per the packaging requirements of the traction inverter. A customized version of laminated busbars by Rogers Corp, Inc, has been shown in figure.4. has improved the power loop inductance to 12 nH [30]. Soldering can be avoided with this type of busbars and thus components can be packed tightly without bondage issues to fit automotive applications.

B. Power Modules

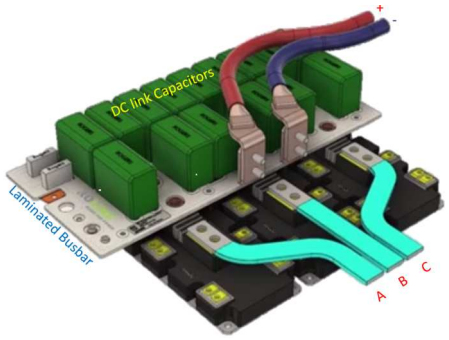

Figure.4. ROLINX CapLink busbars customized for WolfSpeed XM3 Power Modules [30].

Power modules should be chosen to have a low ringing effect in switching voltages, capable of operating at higher switching frequency to output higher fundamental frequencies, higher rated current, and voltage to meet the DoE targets. Over-current, over-voltage, and temperature sense terminals on the power module would be an advantage while packing the components [30]. Overall form factor including the gate driver must be chosen to have high to meet the power-dense targets [31].

C. Capacitors

Capacitors must be selected to have high ripple absorption considering the influence of spatial harmonics during motoring and regeneration mode. The volumetric size and weight of the capacitor must be minimum to meet the VPD, and GPD targets. A proper form factor of the capacitor also influences the overall package of the traction inverter. Bondage failures due to improper soldering can be avoided by screw-type capacitors that would fit on customized busbars. Polypropylene capacitors of coax type made by KEMET C4DE series [32],

Fischer & Tausche, and EPCOS [33] offer higher peak ripple absorption, lightweight and compact in size would fit well for automotive applications.

D. Microcontroller

The microcontroller should possess a higher clock speed to process the currents, speed, and torque simultaneously at higher sampling rates. The multiple numbers of PWM channels would be much-needed requirements in the case of HEV and PHEV where two inverters are needed to drive the motor and generator. It should be able to higher switching frequency. Most of the automakers listed in TABLE.2., have used a 32-bit microcontroller to drive the traction inverter [2].

E. Coolant

Traction inverters need liquid cooling to drive the traction motor rated for several kW. Glycol, Ethylene, and Water, or a combination of these have to be pumped through cooling plates to regulate the temperature of power modules under heavy duty. Micro-finned cooling plates would improve the surface contact with power modules, and can efficiently absorb the heat. Double-sided cooling over single-sided cooling may enhance the cooling capacity and improves the VPD and GPD. A Wolfspeed product of dual inverter for traction applications has been shown in the figure. 5, packed with double-sided cooling enhanced the power density to 72.5 kW/L [34].

Figure.5. XM3 Dual power core inverter by Wolfspeed with micro-finned cooling pate technology [34].

IV. CONCLUSION

State of the art and trends in design specifications of commercially available traction inverters have been reviewed. Key specifications of the traction inverters employed in battery-operated electric vehicles (BEV), plug-in hybrid electric vehicles (PHEV), and hybrid electric vehicles have been reviewed. A trend in volumetric power density (VPD) and gravimetric power density (GPD) of the traction inverters have been landscaped. From the trend, it has been observed that the GPD and the VPD of traction inverters have increased significantly over the past few years. The basic topology of the traction inverter and control methodology that includes MTPA, FWA, and MTPV control algorithms have been reviewed. The selection of various components to design traction inverters to meet VPD and GPD targets has been discussed.

Packaging of the traction inverter involves various components of different electrical, thermal, and mechanical characteristics. An optimized design of the traction inverter needs interdisciplinary contribution from various fields of the research domain to understand the behavior of components under extreme operating conditions from different perspectives. The lack of availability of multiphysics simulation software tools to efficiently pack several components of the traction inverters must be explored further to ease the optimization process.

ACKNOWLEDGMENT

This project was supported by an award from the U.S. Department of Energy Vehicle Technologies Office. The views expressed in the article do not necessarily represent the views of the U.S. Department of Energy or the United States Government.

REFERENCES

[1] “Electrical and Electronics Technical Team Road Map,” U.S. Drive Partnership, Oct. 2017.

[2] “Comparing 10 Leading EV Motors: Webcast,” Virtual Conference on Charged EV Engineering, July 2020.

[3] J. Liu, M. Anwar, P. Chiang, S. Hawkins, Y. Jeong, F. Momen, S. Poulos, and S. Song, “Design of the Chevrolet Bolt EV Propulsion System,” SAE International Journal of Alternative Power Trains, Vol. 5, pp. 79-86, May 2016.

[4] Tim Burress, “Electrical Performance, Reliability Analysis, and Characterization,” DoE VTO Annual Merit Review, June 2017.

[5] J. Reimers, L. Dorn-Gomba, C. Mak, A. Emadi, “Automotive Traction Inverters: Current Status and Future Trends”, IEEE Transaction on Vehicular Technology, Vol.68, No.4, pp. 3337-3350, April 2019.

[6] Tim Burress, “Benchmarking of Competitive Technologies,” DoE VTO Annual Merit Review, Washington, D.C, May 2011.

[7] T. Burress, “Evaluation of the 2007 Toyota Camry Hybrid Synergy Drive System,” Oak Ridge National Laboratory, 2008.

[8] A. Krings and C. Monissen, "Review and Trends in Electric Traction Motors for Battery Electric and Hybrid Vehicles," 2020 International Conference on Electrical Machines (ICEM), pp. 1807-1813, Aug 2020.

[9] S. J. Rind, Y. Ren, Y. Hu, J. Wang, and L. Jiang, "Configurations and control of traction motors for electric vehicles: A review," in *Chinese Journal of Electrical Engineering*, vol. 3, no. 3, pp. 1-17, December 2017.

[10] E. A. Grunditz and T. Thiringer, "Performance Analysis of Current BEVs Based on a Comprehensive Review of Specifications," in IEEE Transactions on Transportation Electrification, vol. 2, no. 3, pp. 270-289, Sept. 2016.

[11] K.T. Chau, Wenlong Li, “Overview of electric machines for electric and hybrid vehicles,” International Journal of Vehicle Design, vol. 74, no.1, pp. 46-71, Sep 2013.

[12] B. Şarlioğlu, "Automotive Power Electronics: Current Status and Future Trends," 2019 International Aegean Conference on Electrical Machines and Power Electronics (ACEMP) & 2019 International Conference on Optimization of Electrical and Electronic Equipment (OPTIM), Feb 2020.

[13] C. Jung, "Power Up with 800-V Systems: The benefits of upgrading voltage power for battery-electric passenger vehicles", *IEEE Electrific. Mag.*, vol. 5, no. 1, pp. 53-58, Mar. 2017.

[14] T. Burress, “Evaluation of the 2010 Toyota Prius Hybrid Synergy Drive System,” Oak Ridge National Laboratory, 2011.

[15] L. Chen and B. Ge, "High Power Traction Inverter Design and Comparison for Electric Vehicles," 2018 IEEE

Transportation Electrification Conference and Expo (ITEC), pp. 583-588, August 2018.
[16] C. Chen, M. Su, Z. Xu and X. Lu, "SiC-based automotive traction drives, opportunities and challenges," 2017 IEEE 5th Workshop on Wide Bandgap Power Devices and Applications (WiPDA), pp. 25-30, 2017.
[17] M. Anwar, M. K. Alam, S. E. Gleason and J. Setting, "Traction Power Inverter Design for EV and HEV Applications at General Motors: A Review," 2019 IEEE Energy Conversion Congress and Exposition (ECCE), pp. 6346-6351, Nov 2019.
[18] Desai, P., Anwar, M., Gleason, S., and Hawkins, S., "Power Electronics for GM 2-Mode Hybrid Electric Vehicles," SAE Technical Paper 2010-01-1253, April 2010.
[19] afford, J., Mazzola, M., Molen, M., Parker, C. et al., "A 1200-V 600-A Silicon-Carbide Half-Bridge Power Module for Drop-In Replacement of an IGBT IPM," SAE Technical Paper 2010-01-1251, April 2010.
[20] Loncarski, Jelena; Leijon, Mats; Srndovic, Milan; Rossi, Claudio; Grandi, Gabriele. 2015. "Comparison of Output Current Ripple in Single and Dual Three-Phase Inverters for Electric Vehicle Motor Drives" *Energies* 8, no. 5: 3832-3848.
[21] M. Niakinezhad, I. U. Nutkani and N. Fernando, "A New Modular Asymmetrical Half-Bridge Switched Reluctance Motor Integrated Drive for Electric Vehicle Application," 2018 IEEE 27th International Symposium on Industrial Electronics (ISIE), pp. 1003-1010, August 2018.
[22] A. S. Lutonin, A. Y. Shklyarskiy and Y. E. Shklyarskiy, "Control Strategy of Dual Fed Open-End Winding PMSM Drive for Traction Applications," 2020 IEEE Conference of Russian Young Researchers in Electrical and Electronic Engineering (EIConRus), pp. 746-749, March 2020.
[23] A. Matsumoto, M. Hasegawa and S. Doki, "A flux-weakening control method on Maximum Torque Control frame for IPMSM position sensorless control," IECON 2012 - 38th Annual Conference on IEEE Industrial Electronics Society, pp. 1612-1617, Dec 2012.
[24] F. Tinazzi, S. Bolognani, S. Calligaro, P. Kumar, R. Petrella and M. Zigliotto, "Classification and review of MTPA algorithms for synchronous reluctance and interior permanent magnet motor drives," 2019 21st European Conference on Power Electronics and Applications (EPE '19 ECCE Europe), pp. P.1-P.10, Nov 2019.
[25] S. Dwivedi, S. M. Tripathi and S. K. Sinha, "Review on Control Strategies of Permanent Magnet-Assisted Synchronous Reluctance Motor Drive," 2020 International Conference on Power Electronics & IoT Applications in Renewable Energy and its Control (PARC), pp. 124-128, May 2020.
[26] Tutorial: Motor Control Design Suite by PSIM, April 2020.
[27] Z. Song, W. Yao and K. Lee, "A V/Hz based Maximum Torque per Volt Control in Flux-Weakening Region for Interior Permanent Magnet Synchronous Motors," 2020 IEEE Energy Conversion Congress and Exposition (ECCE), pp. 2740-2745, Oct 2020.
[28] Tutorial: Design of high perofrmance PMSM Motor Drives, April 2020.
[29] Z. Chen, D. Boroyevich and R. Burgos, "Experimental parametric study of the parasitic inductance influence on MOSFET switching characteristics," The 2010 International Power Electronics Conference - ECCE ASIA -, Sapporo, pp. 164-169, June 2010.
[30] M. Feurtado et al., "High-Performance 300 kW 3-Phase SiC Inverter Based on Next Generation Modular SiC Power Modules," PCIM Europe; International Exhibition and Conference for Power Electronics, Intelligent Motion, Renewable Energy and Energy Management, Nuremberg, Germany, pp. 1-8, July 2019.
[30] Application Note: XM3 Mounting Guide, https://www.wolfspeed.com/downloads/dl/file/id/1503/product/482/xm3_mounting_guide.pdf
[31] Application Note: Evaluation Gate Driver Tool Optimized for the XM3 Module Platform
[32] https://content.kemet.com/datasheets/F3303_C4DE.pdf
[33] https://www.ftcap.de/fileadmin/user_upload/download_inhalte/Katalog_FIKO_Web.pdf
[34] Webinar:Unlock Higher Power Density in Motor Drives using SiC Modules: